

Pulsed laser deposition of Ni thin films on Si (100) and flexible PDMS substrates

F. STOKKER-CHEREGI*, D. COLCEAG, M. FILIPESCU, V. ION, A. PALLA-PAPAVLU,
A. VLAD, M. DINESCU

National Institute for Lasers, Plasma, and Radiation Physics, 077125 Magurele, Romania

**Corresponding author: flavian.stokker@inflpr.ro*

Received September 29, 2017

Abstract. The field of microfluidic devices for real-time polymerase chain reaction analysis has seen significant advances during the last years. Our study of Ni thin films grown on polydimethylsiloxane (PDMS) substrates was triggered by the perspective of using and integrating such structures in future on-chip DNA amplification devices. The thin films were obtained by pulsed laser deposition from a Ni target onto Si and PDMS supports. The samples were characterized mainly from a structural, morphological, compositional, and optical point of view. Initial electrical measurements, at low currents, revealed that the stripes exhibit resistance values of the order of 100 ohms.

Key words: PLD, Ni thin films, PDMS, flexible substrates.

1. INTRODUCTION

The field of modern microfluidics has grown to be extremely vast; with its complexity stemming both from the wide range of specific applications addressed by microfluidic devices, as well as from the solutions proposed to achieve the respective functionalities. The ultimate goal of most studies is the realization of lab-on-a-chip (LOC) systems [1, 2], which are complex devices, of reduced dimensions, that are able to perform several complementary tasks. The applications for such devices are primarily oriented towards biomedicine [3], and they include: polymerase chain reaction analysis [4-10], cell separation [11, 12], digital microfluidics [13-16], mixing [17] etc..

In virtually all such applications, one of the key elements in mimicking operations performed by standard laboratory equipment, such as microarrays [18], is the control of heating protocols required by the respective biochemical

processes. During the last decade, many such heating/cooling technologies have been proposed to be used in microfluidic devices. For example, some of these approaches rely on a pre-heating of the liquid [4], and therefore they are not performed within the actual chip. In many such instances an external thermal reservoir is used in order to try and regulate the temperature gradient within the chip that is placed in contact with the heater [19, 20]. The fact that these solutions are not integrated into one device gives rise to certain constraints on their potential fields of applications, and therefore many research groups are rather pursuing the development of integrated technologies for LOC systems. These include the use of Joule heating [10, 15, 21], laser heating [22], microwaves [23, 24] etc.

Despite of the remarkable progress achieved towards the development of microfluidic systems, the obtained solutions have rarely made it into commercial applications. One of the main reasons for this shortcoming is the complexity of these devices, which often translates into elevated production costs. The use of external heaters was indeed considered in order to make the chips more facile to manufacture [19], but at the same time limiting their capabilities. In the case of the more versatile device integrated heaters, a solution needs to be found for cheap, robust, and easy to manufacture temperature control systems. This work represents a first step in our effort to address these issues through the growth of Ni thin film stripes on flexible polydimethylsiloxane (PDMS) substrates by pulsed laser deposition (PLD) to help in designing new thin films heater system. PLD is an old technique, which has been used extensively starting 1965, when Smith and Turner deposited the first thin films using a ruby laser. Briefly, PLD involves the interaction of a laser beam with a target material resulting in a plume that is transporting the ablated species to a substrate, where a thin film is formed [25-30].

We stress out the fact that the obtaining of integrated heating elements that are cheap, robust and flexible at the same time is non-trivial. In many cases, the proposed solutions do not fulfill all these requirements, thus limiting their use. Such has been the case of epoxy heaters on PDMS having reduced flexibility [21] or the degrading of Al thin films heaters [31].

2. EXPERIMENTAL

In order to achieve optimal surface morphology and crystallographic properties for the Ni thin films on PDMS substrates, a parametric study was first carried out. The Ni thin films were obtained using a classical PLD setup by ablating a Ni target (purity >99.99%) with a “Surelite II” pulsed Nd:YAG laser system (Continuum Company).

In addition to the flexible PDMS substrates (1 cm² samples), rigid Si (100) cut into 1 cm² substrates polished on both sides were also employed to collect the ablated material. Both types of substrates, i.e. the Si and PDMS were cleaned in successive baths of acetone, ethanol, and double distilled water prior to the depositions. Many different growth parameters were varied during our initial parametric study. Two wavelengths were considered for the ablation laser source: 355 and 532 nm, respectively. The pulse repetition rate was 10 Hz for all samples, however the pulse energy and spot sizes were varied between 9 and 36 mJ and 0.3 - 0.9 cm², respectively, thus resulting in laser fluences between 1.5 and 4.8 J/cm². The number of pulses delivered to the target in these experiments was between 36,000 and 144,000.

The Ni thin films were obtained in vacuum (10⁻⁵ mbar). The distance between target and substrate was initially set at 6 cm, but ultimately it was lowered to 4 cm in order to compensate for the poor deposition rate of Ni. Most of the samples were grown at room temperature (RT), although some attempts were made to grow at substrate temperatures up to 200 °C in order to smooth out morphological irregularities. This, however, gave rise to a non-negligible surface oxidation of the samples, and therefore the best performing samples were obtained at RT.

The morphology of the deposited Ni thin films was investigated by atomic force microscopy (AFM) using a XE100 Park instrument operated in non-contact mode. The surface roughness of the films was investigated on several different areas and dimensions from 5×5 μm² to 40×40 μm². In addition, AFM measurements were carried out to determine the thickness of the deposited thin films. XRD measurements were performed in Bragg-Brentano geometry ($\theta - 2\theta$, between 35° and 60°) using a PANalytical X'Pert PRO MRD diffractometer.

Spectroellipsometry (SE) was used to cross-check material characteristics obtained from XRD results and also to infer information about film thickness. Optical measurements were carried out with a Woollam Variable Angle SE (VASE) system, equipped with a high pressure Xe discharge lamp incorporated in an HS-190 monochromator.

A secondary ion mass spectrometry (SIMS) system, from Hidden Analytical, was used to probe the surface and in-depth element composition of the Ni thin films. Finally, preliminary conductivity measurements at low currents were carried out on the Ni thin film stripes grown on PDMS substrates using a digital multimeter.

3. RESULTS AND DISCUSSION

In this work we will discuss three sets of selected samples that were of the highest quality, prepared following our parametric study. Some of the experimental conditions under which the Ni thin films were processed are common to all three samples, and they include: 532 nm laser ablation wavelength, 10 Hz pulse repetition rate, spot area of 0.75 mm², Ni target to substrate distance of 4 cm, residual atmosphere of 10⁻⁴ mbar, and substrate kept at room temperature. Other growth parameters that are not common to all samples have been summarized in Table I.

Sample	Collector	No. of pulses	E _{laser} (mJ)	Laser fluence (J/cm ²)
A	Si (100) + PDMS	36,000	18	2.4
B	Si (111) + PDMS	36,000	36	4.8
C	PDMS with mask	144,000	36	4.8

Table I. Growth conditions of selected samples.

Although the films deposited on PDMS are more relevant in view of the perspective applications, the growth of Ni films on Si substrates was also chosen either in order to alleviate constraints imposed by specific analysis techniques, such as SIMS and ellipsometry, or to render the analysis and interpretation of results more straightforward, as in the case of XRD.

The AFM images of samples A (top) and B (bottom) on areas of 40 × 40 μm, for both types of substrates are shown in Fig. 1. The Ni thin films grown on Si substrates exhibit considerably lower roughness values, of the order of tens of nm, as compared to those obtained on PDMS supports, which have roughness values exceeding 100 nm. The origin of this large difference resides in the intrinsic nature of the PDMS substrate surface, which exhibits a ridged like morphology. Although the ridged aspect of the substrate greatly alters the morphology of the samples grown on PDMS, Ni films grown on both types of substrates are continuous, and without cracks.

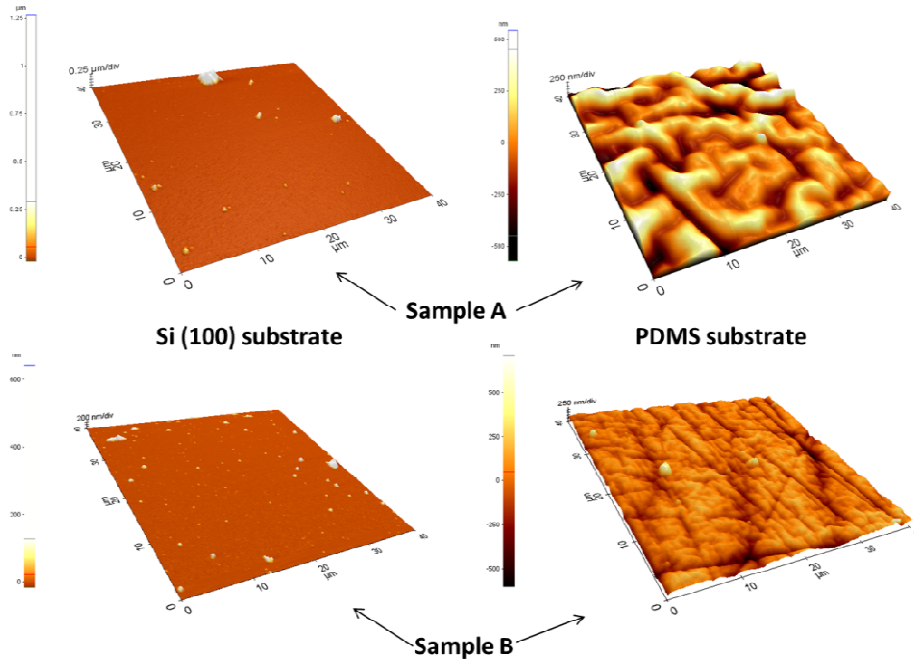


Fig. 1 – AFM images over areas of $40 \times 40 \mu\text{m}$ of sample A (top) and sample B (bottom) grown on Si (left) and PDMS (right) substrates, respectively.

Spectroscopic ellipsometry measurements were acquired in the 300-1700 nm spectral range, with a step of 2 nm and the beam incident at an angle of 70° . The optical constants (n and k) are not measured directly in ellipsometry, instead they are deduced from the polarization change in amplitude ratio (Ψ) and phase difference (Δ) of the incident radiation as a result of its interaction with the material of interest. In order to quantify n and k , certain assumptions need to be made about the thickness and roughness of the obtained films. In our case, each of the two samples was fitted with a 3-layer model, which assumed: i) the Si substrate; ii) a native layer of SiO_2 having a thickness of 3 nm; and iii) the top Ni film. The refractive index (n) and extinction coefficients (k) inferred from the ellipsometry data are shown in Fig. 2, and compared to a reference from the SE database [32].

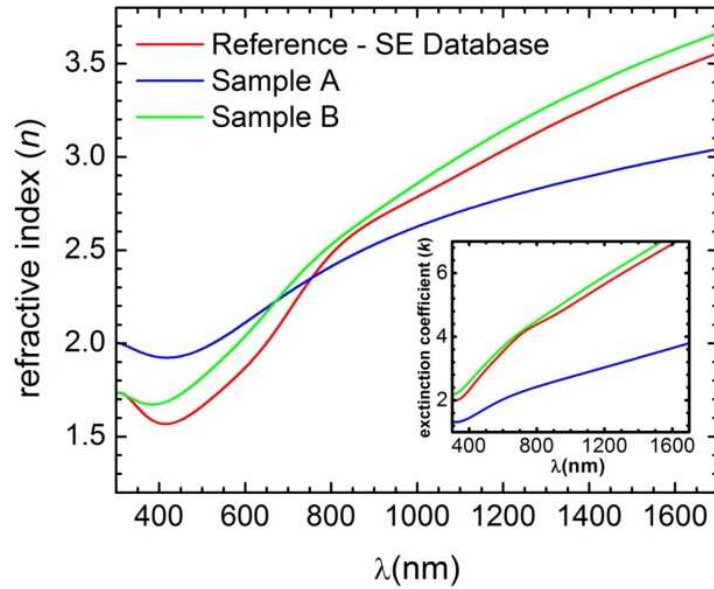


Fig. 2 – Refractive indexes and extinction coefficients (inset) determined from spectroellipsometry measurements for samples A and B, as compared to the values of Ni from ref. [32].

One straightforward observation is that the optical constants for sample B are in good agreement with theory, whereas sample A exhibits a marked departure from these values. This discrepancy originates from the fact that these films have thicknesses of the order of tens of nanometers, which tend to be about the same order of magnitude as their respective roughness. More specifically, the Ni film on sample A was determined to have a thickness of 30 nm, whereas on sample B it is about 60 nm thick. However, the roughness of sample A was determined to be around 40 nm, whereas that of sample B is only 20 nm. Therefore, the roughness of sample A will impact its optical properties to a larger extent, thus explaining the differences of optical constants with respect to the reference values.

The low thickness of sample A also made it very difficult to achieve a reliable characterization of its crystalline quality by XRD. This is why in Fig. 3 only the diffractograms for sample B; both on Si and PDMS substrates are displayed. For the Si substrate, the spectrum was acquired using a 1 degree offset of the incident beam in order to cancel out substrate contributions. This was not necessary for the Ni film grown on PDMS, and therefore the diffractogram of this particular sample exhibits improved signal-to-noise ratio. Sample B on PDMS exhibits the two highest intensity characteristic peaks assignable to the Ni cubical

system, namely the (111) and (200) reflections, in agreement with the PDF card #00-004-0850. This is a first indication that our obtained films are of pure Ni, without the presence of NiO which would have negatively impacted their functional properties.

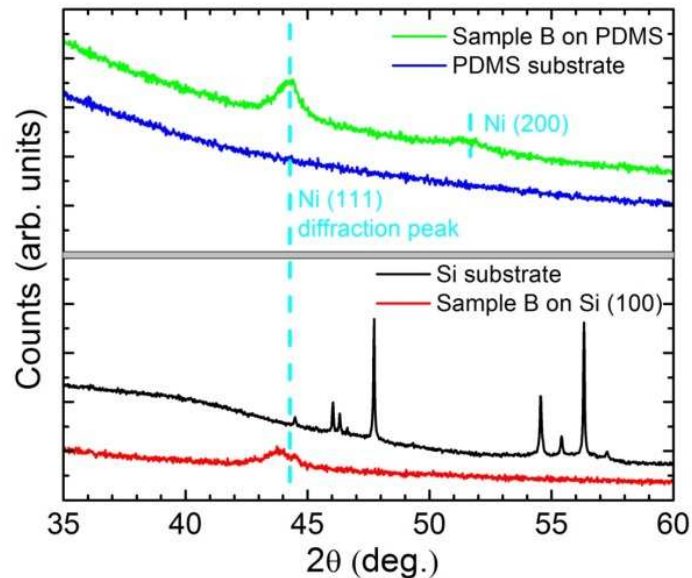


Fig. 3 – Diffractograms of sample B grown on PDMS (top) and Si (bottom), as compared to the respective substrates. The spectra are shifted in intensity for clarity.

The SIMS analyses shown in Fig. 4 were performed on the samples grown on Si substrates in order to check their in-depth homogeneity and composition. In the case of sample A, there are significant fluctuations in the depth profile of the Ni film. This agrees well with AFM results that showed high roughness values, and it also helps explain the different optical constants measured by SE for this sample, as compared to those expected from theory. On the other hand, the depth profile of the Ni thin film in sample B shows very little variations, which once again agrees with AFM and SE results. For both samples, the interfaces are sharp, with negligible inter-diffusion of elements between the deposited Ni films and the substrate. The mass scan in the inset of sample B reveals that the film does not contain impurities, and is composed mainly of the two isotopes of Ni (^{58}Ni and ^{60}Ni), in their respective natural abundances. The other elements discernable in the mass scan are the Si substrate and the ones originating from the instrumental background.

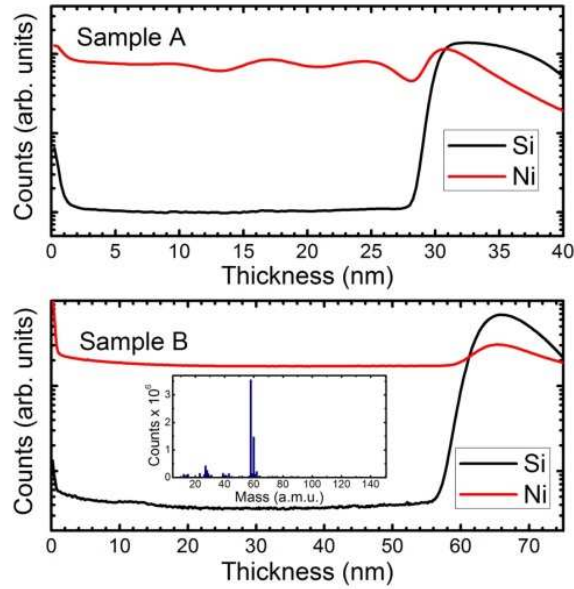


Fig. 4 – Depth profile of Ni and Si elements for sample A (top) and sample B (bottom) grown on Si (100) substrates. The inset in the plot of sample B is a mass scan of the respective thin film.

All of the undertaken analyses have ultimately revealed the superior quality of sample B, with respect to sample A, in terms of morphology, in-depth homogeneity and optical properties. However, resistivity measurements on these samples showed resistance values of the order of 10-20 ohms. Such resistance values are rather low when considering the tentative applications for these layers as heaters relying on the Joule effect. As a consequence, sample C was obtained using four times the number of pulses applied for sample B in order to increase the Ni film cross-section, and hence its resistance. Sample C was grown by applying a mask to the PDMS substrate, thus achieving the growth of three identical stripes having sizes of 13 x 3 mm, with 2 mm spacing between adjacent stripes, as illustrated in Fig. 5.

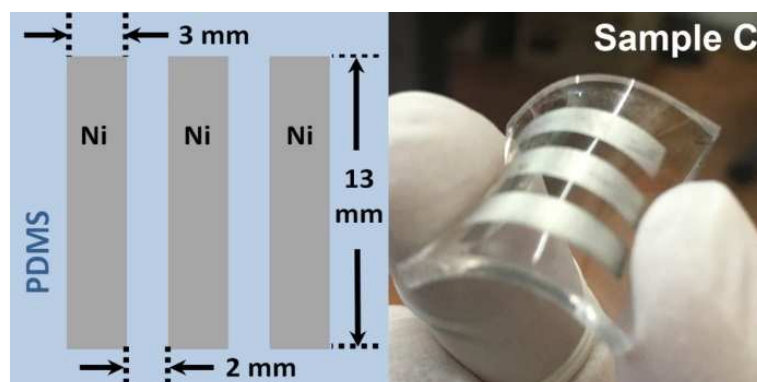


Fig. 5 – Schematic representation of the layout (left) and photo (right) of sample C.

The electrical resistance of each stripe on sample C was determined to be around 100 ohms, a value that shows potential towards the development of thin films based heaters for microfluidic devices [33]. Our sample was developed with the specific aim to resolve issues related to robustness, miniaturization and ease of processing. Therefore, sample C was also subjected to tens of bending cycles, which did not cause a degradation of its electrical properties. These results indicate that our Ni thin film stripes show great potential towards integration in more complex microfluidic devices, a task which we will undertake in our upcoming studies.

4. CONCLUSIONS

In the present work we have taken the first steps towards finding a cheap, robust and miniaturized solution that addresses some of the issues of microfluidic devices with Joule effect based heating, such as reduced flexibility [21] or heater degradation [31].

Our parametric study of Ni thin films growth on Si and PDMS substrates allowed us to determine the optimal growth parameters for high quality Ni thin films having good adherence and coverage of their respective substrates. XRD measurements reveal the achievement of a pure Ni phase, without the presence of NiO. In addition, the films obtained using a laser fluence of 4.8 J/cm^2 show improved optical parameters and in-depth homogeneity, with respect to those processed at 2.4 J/cm^2 . The higher fluence was also used to process Ni thin film stripes having resistance values of around 100 ohms, which makes them suitable for use in microfluidic devices [33]. Due to their excellent robustness, the electrical

properties of the Ni/PDMS constructs are preserved over tens of bending cycles, and therefore in our subsequent studies they will be used in the realization of microfluidic devices.

Acknowledgements. This work was supported by the National Program 4N/2016, and grants of the Romanian National Authority for Scientific Research and Innovation, CNCS – UEFISCDI, project number PNII-PT-PCCA-2013-4-1992 (SOLE) and PN-II-RU-TE-2014-4-2311 (FLEXsens).

REFERENCES

1. D. Mark, St. Haeberle, G. Roth, F. von Stetten, R. Zengerle, Microfluidic lab-on-a-chip platforms: requirements, characteristics and applications, *Chem. Soc. Rev.* **39**, 1153 (2010).
2. S. Haeberle, R. Zengerle, Microfluidic platforms for lab-on-a-chip applications, *Lab Chip* **7**, 1094 (2007).
3. E.K. Sackmann, A.L. Fulton, D.J. Beebe, The present and future role of microfluidics in biomedical research, *Nature* **507**, 18 (2014).
4. G. Maltezos, M. Johnston, K. Taganov, C. Srichantaratsamee, J. Gorman, Exploring the limits of ultrafast polymerase chain reaction using liquid for thermal heat exchange: A proof of principle, *Appl. Phys. Lett.* **97**, 264101 (2010).
5. Z. Hua, J.L. Rouse, A.E. Eckhardt, V. Srinivasan, V.K. Pamula, W.A. Schell, J.L. Benton, T.G. Mitchell, M.G. Pollack, Multiplexed real-time polymerase chain reaction on a digital microfluidic platform, *Anal. Chem.* **82**, 2310 (2010).
6. M.P. Dinca, M. Gheorghe, M. Aherne, P. Galvin, Fast and accurate temperature control of a PCR microsystem with a disposable reactor, *J. Micromech. Microeng.* **19**, 065009 (2009).
7. K.Y. Lien, S.-H. Lee, T.-J. Tsai, T.-Y. Chen, G.-B. Lee, A microfluidic-based system using reverse transcription polymerase chain reactions for rapid detection of aquaculture diseases, *Microfluid. Nanofluid.* **7**, 795 (2009).
8. X. Qiu, M.G. Mauk, D. Chen, C. Liu, H.H. Bau, A large volume, portable, real-time PCR reactor, *Lab Chip* **10**, 3170 (2010).
9. T.-M. Hsieh, C.-H. Luo, J.-H. Wang, J.-L. Lin, K.-Y. Lien, G.-B. Lee, Enhancement of thermal uniformity for a microthermal cyler and its application for polymerase chain reaction, *Microfluid. Nanofluid.* **6**, 797 (2009).
10. J.-H. Wang, L.-J. Chien, T.-M. Hsieh, C.-H. Luo, W.-P. Chou, P.-H. Chen, P.-J. Chen, D.-S. Lee, G.-B. Lee, A miniaturized quantitative polymerase chain reaction system for DNA amplification and detection, *Sens. Actuator. B* **141**, 329 (2009).
11. T. Matsui, J. Franzke, A. Manz, D. Janasek, Temperature gradient focusing in a PDMS/glass hybrid microfluidic chip, *Electrophoresis* **28**, 4606 (2007).
12. D. Ross, L.E. Locascio, Microfluidic temperature gradient focusing, *Anal. Chem.* **74**, 2556 (2002).

13. Y.F. Yap, S.H. Tan, N.T. Nguyen, S.M.S. Murshed, T.N. Wong, L. Yobas, Thermally mediated control of liquid microdroplets at a bifurcation, *J. Phys. D Appl. Phys.* **42**, 1 (2009).
14. A.A. Darhuber, J.P. Valentino, S.M. Troian, Planar digital nanoliter dispensing system based on thermocapillary actuation, *Lab Chip* **10**, 1061 (2010).
15. B. Selva, V. Miralles, I. Cantat, M.-C. Jullien, Thermocapillary actuation by optimized resistor pattern: bubbles and droplets displacing, switching and trapping, *Lab Chip* **10**, 1835 (2010).
16. M.T. Guo, A. Rotem, J. A. Heyman, D.A. Weitz, Droplet microfluidics for high-throughput biological assays, *Lab Chip* **12**, 2146 (2012).
17. S.-J. Kim, F. Wang, M.A. Burns, K. Kurabayashi, Temperature-programmed natural convection for micromixing and biochemical reaction in a single microfluidic chamber, *Anal. Chem.* **81**, 4510 (2009).
18. B.-X. Hong, L.-F. Jiang, Y.-S. Hu, D.-Y. Fang, H.-Y. Guo, Application of oligonucleotide array technology for the rapid detection of pathogenic bacteria of foodborne infections, *J. Microbiological Methods* **58**, 403 (2004).
19. K.T.L. Trinh, W. Wu, N.Y. Lee, Planar poly(dimethylsiloxane) (PDMS)–glass hybrid microdevice for a flow-through polymerase chain reaction (PCR) employing a single heater assisted by an intermediate metal alloy layer for temperature gradient formation, *Sens. Actuator. B* **190**, 177 (2014).
20. W. Wu, N.Y. Lee, Three-dimensional on-chip continuous-flow polymerase chain reaction employing a single heater, *Anal. Bioanal. Chem.* **400**, 2053 (2011).
21. D. Vigolo, R. Rusconi, R. Piazza, H.A. Stone, A portable device for temperature control along microchannels, *Lab Chip* **10**, 795 (2010).
22. H. Kim, S. Vishniakou, G.W. Faris, Petri dish PCR: Laser-heated reactions in nanoliter droplet arrays. *Lab Chip* **9**, 1230 (2009).
23. G. Yaralioglu, Ultrasonic heating and temperature measurement in microfluidic channels, *Sens. Actuator. A* **170**, 1 (2011).
24. J.J. Shah, J. Geist, M.A. Gaitan, Microwave-induced adjustable nonlinear temperature gradients in microfluidic devices, *J. Micromech. Microeng.* **20**, 105025 (2010).
25. J. Schou, Physical aspects of the pulsed laser deposition technique: The stoichiometric transfer of material from target to film, *Appl. Surf. Sci.* **255**, 5191, (2009).
26. D.B. Chrisey, A. Piqué, R.A. McGill, J.S. Horwitz, B.R. Ringeisen, D.M. Bubb, P.K. Wu, Laser Deposition of Polymer and Biomaterial Films, *Chem. Rev.* **103** (2), 553–576, (2003).
27. A. Palla-Papavlu, M. Filipescu, C.W. Schneider, S. Antohe, P.M. Ossi, G. Radnóczy, M. Dinescu, A. Wokaun, T. Lippert, Direct laser deposition of nanostructured tungsten oxide for sensing applications, *J. Phys. D: Appl. Phys.* **49**, 205101 (2016).

28. A. Palla-Papavlu, V. Dinca, V. Ion, A. Moldovan, B. Mitu, C. Luculescu, M. Dinescu, Characterization of polymer thin films obtained by pulsed laser deposition, *Appl. Surf. Sci.* **257**, 5303–5307 (2011).
29. J. Chen, A. Palla-Papavlu, Y. Li, L. Chen, X. Shi, M. Dobeli, D. Stender, S. Populoh, W. Xie, A. Weidenkaff, C.W. Schneider, A. Wokaun, T. Lippert, Laser deposition and direct-writing of thermoelectric misfit cobaltite thin films, *Appl. Phys. Lett.* **104**, 2319107 (2014).
30. F. Stokker-Cheregi, A. Nedelcea, F.M. Voicu, D.M. Marin, R. Birjega, M. Dinescu, Structure and morphology of indium nitride thin films grown by plasma assisted PLD: The impact of nitrogen flow and substrate temperature, *Rom. Rep. Phys.* **65**, 213 (2013).
31. J. Martinez-Quijada, S. Caverhill-Godkewitsch, M. Reynolds, L. Gutierrez-Rivera, R.W. Johnstone, D.G. Elliott, D. Sameoto, C.J. Backhouse, Fabrication and characterization of aluminum thin film heaters and temperature sensors on a photopolymer for lab-on-chip systems, *Sens. Actuator. A* **193**, 170 (2013).
32. E.D. Palik, G. Ghosh, *Handbook of Optical Constants of Solids*, Academic Press (1998).
33. V. Mirales, A. Huerre, F. Malloggi, M.-C. Jullien, A Review of Heating and Temperature Control in Microfluidic Systems: Techniques and Applications, *Diagnostics* **3**, 33 (2013).